



# Fast Monte Carlo simulation for particle coagulation in population balance



Zuwei Xu, Haibo Zhao\*, Chuguang Zheng

State Key Laboratory of Coal Combustion, Huazhong University of Science and Technology, Wuhan 430074, Hubei, PR China

## ARTICLE INFO

### Article history:

Received 20 May 2013

Received in revised form

14 December 2013

Accepted 21 March 2014

Available online 18 April 2014

### Keywords:

Population balance modeling

Particle coagulation

Stochastic simulation

Differentially weighting scheme

Particle size distribution

## ABSTRACT

The Monte Carlo (MC) method for population balance modeling (PBM) has become increasingly popular because the discrete and stochastic nature of the MC method is especially suited for particle dynamics. However, for the two-particle events (typically, particle coagulation), the double looping over all simulation particles is required in normal MC methods, and the computational cost is  $O(N_s^2)$ , where  $N_s$  is the simulation particle number. This paper proposes a fast random simulation scheme based on the differentially-weighted Monte Carlo (DWMC) method. The majorant of coagulation kernel was introduced to estimate the maximum coagulation rate by a single looping over all particles rather than the double looping. The acceptance–rejection process then proceeded to select successful coagulation particle pairs randomly, and meanwhile the waiting time (time-step) for a coagulation event was estimated by summing the coagulation kernels of rejected and accepted particle pairs. In such a way, the double looping is avoided and computational efficiency is greatly improved as expected. Five coagulation cases for which analytical solutions or benchmark solutions exist were simulated by the fast and normal DWMC, respectively. It is found the CPU time required is orders of magnitude lower and only increases linearly with  $N_s$ ; at the same time the computational accuracy is guaranteed very favorably.

© 2014 Elsevier Ltd. All rights reserved.

## 1. Introduction

Coagulation between particles (or bubbles, droplets) is ubiquitous in many different fields of nature and engineering (Friedlander, 2000), including atmospheric physics (aerosol dynamics), combustion (the growth of particulate matter, soot and PAH), chemical engineering (e.g., polymerization, granulation, crystallization, and precipitation), catalytic chemical processes, food processes, nanoparticle synthesis, and so on. The particle coagulation refers to two particles collide and adhere together, leading to the increase of average particle size and the decrease of particle number concentration, i.e., the dynamic evolution of particle size distribution (PSD). Among the various particle dynamic events, coagulation is the most demanding event for modeling, as it always involves two discrete particles. The population balance equation (PBE) for particle coagulation, which characterizes coagulation dynamics in term of the time evolution of PSD, is represented by the following mathematical equation:

$$\frac{\partial n(v, t)}{\partial t} = \frac{1}{2} \int_{v_{\min}}^v \beta(v-u, u, t) n(v-u, t) n(u, t) du - n(v, t) \int_{v_{\min}}^{v_{\max}} \beta(v, u, t) n(u, t) du. \quad (1)$$

\* Corresponding author. Tel.: +86 27 87542417 8208; fax: +86 27 87545526.

E-mail address: [klinsmannzhb@163.com](mailto:klinsmannzhb@163.com) (H. Zhao).

where  $n(v, t)$  with dimension  $m^{-3} m^{-3}$  is the particle size distribution function (PSDF) at time  $t$ , so that  $n(v, t)dv$  is the number concentration of particles with size range between  $v$  and  $v+dv$  at time  $t$ ;  $\beta(v, u, t)$  is the coagulation kernel for two particles of volumes  $v$  and  $u$  at time  $t$ ,  $m^3 s^{-1}$ .

Because of the partial integro-differential nature of the PBE, it is difficult to solve it directly. Only for a few ideal cases can we get analytic solutions, otherwise we can only get approximate solutions by numerical methods. The deterministic scheme such as sectional method and method of moments (Frenklach & Harris, 1987; Gelbard et al., 1980) is capable of solving Eq. (1) either through an appropriate discretization scheme or by quadrature. However, there exist some difficulties such as complicated mathematical models (especially for multivariate population balance) and discrete errors for the deterministic methods. The stochastic (Monte Carlo) scheme, which describes directly the dynamic evolution of particle population in dispersed systems, approximates the PBE solution through a large amount of random sampling from the system. The discrete nature of the MC method adapts itself naturally to the discrete process (i.e., the discrete particle population and the discrete dynamic events). The population balance-Monte Carlo (PBMC) can obtain the details of the dynamic evolution of multi-dimensional, multi-component, and polydispersed particle population (Zhao & Zheng, 2011, 2013; Zhao et al., 2011). Furthermore, the MC algorithm is comparatively easy to program. Owing to these advantages, MC constitutes an important class of methods for the numerical solution of the population balance modeling (PBM).

Generally speaking, MC methods can be classified either by time discretization scheme into event-driven MC and time-driven MC, or by simulation particle weighting scheme into equally-weighted MC and differentially-weighted MC. Event-driven MC (Garcia et al., 1987) first calculates time interval (or waiting time)  $\Delta t_{ED}$  between two successive events based on the average rate of event processes and then uses the stochastic game to choose the event that happens after this waiting time. Time-driven MC (Liffman, 1992) considers all possible events that may happen within a pre-specified time step  $\Delta t_{TD}$  to be decoupled;  $\Delta t_{TD}$  is constrained to be less than or equal to the minimum time scale within which each simulation particle participates in one coagulation event at most. Most of the MC methods (Garcia et al., 1987; Liffman, 1992; Lin et al., 2002; Maisels et al., 2004) belong to the equally-weighted method, in which all simulation particles have the same weight. Usually a subsystem of the total system is simulated either explicitly or implicitly, in which the common weight is equal to the ratio of the volume of the total system to that of the subsystem. However, the equally weighting scheme leads to a great deal of statistical noise for particles in those less-populated sections such as at the edges of log-normal distributed size spectrum. In the differentially weighting scheme, these sections where the number density is low can be represented by simulation particles with appropriate number and relatively small weight. Keeping track of differentially weighted simulation particles of different sizes will thus help to improve the accuracy of MC. We have proposed the differentially-weighted Monte Carlo (DWMC) method for particle coagulation for univariate population balance (Zhao et al., 2005a, 2005b) and multivariate population balance (e.g., two-component aggregation) (Zhao et al., 2010, 2011). The key ideas are to establish the coagulation rules that describe how to deal with coagulation between differentially-weighted simulation particles, and to specify how the simulation particles should be homogeneously distributed over the size spectrum (rather than to let them evolve freely). The DWMC can evolve in either event-driven mode (Zhao & Zheng, 2009b) or time-driven mode (Zhao et al., 2010), and keeps the total number of simulation particles constant in simulation. It was validated that the DWMC methods perform better statistical accuracy than other equally-weighted MC.

It is worth emphasizing that an optimal combination of high accuracy and high efficiency are essential for PBMC, because with the increase in simulation particle number its numerical accuracy increases while its computational efficiency decreases. For the two-particle events such as coagulation (or aggregation, agglomeration), the normal PBMC simulation has to calculate/update the interaction probability of any particle pair each time step to obtain probability distribution of random events and the waiting time between two successive events. The double looping over all simulation particles is thus required in the normal PBMC methods, so the computational cost reaches  $O(N_s^2)$ , where  $N_s$  is the simulation particle number. Although there is dramatic increase in computational power over the past decade, it is still very necessary to improve the computational efficiency for fast prediction of particle dynamics. There are two kinds of ways to accelerate MC simulation: one is parallel computing (Kruis et al., 2010), including CPU parallel computing based on Message Passing Interface (MPI) and Open Multi-Processing (OpenMP), and Graphitic Processing Unit (GPU) parallel computing based on Open Computing Language (OpenCL) and Compute Unified Device Architecture (CUDA) (Wei & Kruis, 2013). Factually the parallel computing of MC simulation uses more computer source simultaneously to reduce computational time. Another is to improve the scheme of PBMC itself to accelerate simulation. Kruis et al. (2000) proposed the smart bookkeeping technology to avoid a large number of re-calculations of the coagulation rates of particles not participating in coagulation, in such a way that the CPU time is greatly saved without loss in accuracy. Wagner et al. (Eibeck & Wagner, 2000, 2001) and Kraft et al. (Goodson & Kraft, 2002) developed a new efficient MC which utilized the majorant of coagulation kernel to calculate the coagulation probability of all particle pairs by a single looping over all particles rather than the double looping. A Markov model with fictitious jumps was then constructed to simulate particle dynamics with high accuracy. The CPU time increases linearly with  $N_s$ , rather than as  $N_s^2$  (as with the conventional MC). Recently, Wei (2013) proposed a fast acceptance–rejection scheme that can boost the performance of Monte Carlo methods for particle coagulation by establishing a connection between the information of particle pairs and the maximum coagulation rate. Lécot and Tarhini (2008) and Lécot and Wagner (2004) proposed the quasi-Monte Carlo to accelerate the convergence rate, in which pseudo-random numbers were replaced by quasi-random numbers or low-discrepancy point sets (which are “evenly distributed”). Similar idea in terms of good lattice point set was also used by Kruis et al. (2012) to estimate the maximum of coagulation kernel with a remarkable gain in efficiency. Another measure accelerating PBMC simulation is to simulate coagulation between particle species rather than

between discrete simulation particles (as with the conventional MC). In the species-based MC, the particles with size in a specified interval are viewed as pseudochemical species, and the stochastic simulation algorithm for chemical kinetics is adopted to define the state of a coagulating system in terms of “coagulation/aggregate species” (Gillespie, 1976). The species-based algorithm had a variety of different implementations by different researchers such as Laurenzi and Diamond (1999), Irizarry (2008a, 2008b), Kraft et al. (Shekar et al., 2012a, 2012b), Debry et al. (2003), DeVille et al. (2011), and Riemer et al. (2009). The species-based MC methods exhibit an excellent improvement in efficiency and memory demand because the number of particle species is usually far less than that of discrete simulation particles. However, their computational accuracy is generally lower than the conventional particle-based MC. Furthermore the species-based MC methods are usually at the cost of complicated algorithms and are less sensitive to the innate fluctuations for coagulation processes which are also stochastic in nature.

To sum up, the above-mentioned measures can improve computational efficiency of PBMC simulation more or less, however, at the cost of either obvious losing in accuracy, or increasing in complexity of PBMC algorithms. This paper aims to improve the simulation scheme of the DWMC method (Zhao et al., 2009, 2010; Zhao & Zheng, 2009b) and then proposes a fast DWMC method, which is expected that the single looping over all simulation particles is just required to simulate particle coagulation dynamics within one time-step. In order to examine the performance of the fast-DWMC method, five special coagulation cases for which analytical solutions (for constant coagulation kernel and linear coagulation kernel) or benchmark solutions (for Brownian coagulation kernels in the free molecular regime and continuum regime) exist are simulated by the fast DWMC and the normal DWMC respectively. Their accuracy and cost are compared and analyzed.

## 2. Theory and method

### 2.1. Normal differentially-weighted MC

The concept of weighting simulation particles is widely utilized by MC to overcome the conflict between large numbers of real particles and limited CPU speed and memory capacity. The weight of a simulation particle  $i$ ,  $w_i$ , means the simulation particle  $i$  represents  $w_i$  real particles having the same or similar internal variables (i.e., size, component) as  $i$ . Note that the size distribution is usually polydisperse in real cases and particle dynamics such as coagulation leads to the dynamic evolution of size distribution. The differentially weighting scheme is especially suited for the inhomogeneous and time-varying characteristics of particle size distribution function.

The key issue of the differentially-weighted MC is to design a rule for coagulation event between two differentially-weighted simulation particles. We introduced probability theory to consider coagulation in pairs. Under the probabilistic coagulation rule, for a coagulation event between simulation particles  $i$  and  $j$  (their weights  $w_i$  and  $w_j$  are unequal); it is imagined that each real particle from  $i$  undergoes a real coagulation event with a probability of  $\min(w_i, w_j)/w_i$ , and each real particle from  $j$  does so with a probability of  $\min(w_i, w_j)/w_j$ . Thus, on average, only  $\min(w_i, w_j)$  real particles from  $i$  or  $j$  participate in real coagulation. As a result, two new simulation particles, which represent “coagulated” real particles and “non-coagulated” real particles respectively, are produced to replace the old simulation particles  $i$  and  $j$ . We formulated the result of a coagulation event as follows:

$$\begin{aligned} w_i^* &= \max(w_i, w_j) - \min(w_i, w_j); & m_i^* &= m_k|_{w_k = \max(w_i, w_j)}; & v_i^* &= v_k|_{w_k = \max(w_i, w_j)}; \\ w_j^* &= \min(w_i, w_j); & m_j^* &= m_i + m_j; & v_j^* &= v_i + v_j; \end{aligned} \quad (2)$$

where the asterisk indicates a new value of weight or state after the coagulation event;  $m_i$  and  $v_i$  are the total mass and volume of simulation particle  $i$  respectively; the particle diameter ( $d$ ) can be obtained from particle volume, assuming the aggregates attain rapidly a spherical shape due to fast coalescence or sintering. It is obvious that Eq. (2) satisfies the laws of conservation of mass, and also keeps the number of simulation particles constant.

As far as the probabilistic coagulation rule is concerned, the total coagulation rate of simulation particle  $i$  ( $C_i'$  with dimension of  $\text{m}^{-3} \text{s}^{-1}$ ), which is the accumulative total of the coagulation rate between  $i$  and any one of the other simulation particles, is calculated as (Zhao et al., 2009)

$$C_i' = \frac{1}{V^2} \sum_{j=1, i \neq j}^{N_s} \left[ \frac{2\beta_{ij} w_j \max(w_i, w_j)}{w_i + w_j} \right] = \frac{1}{V^2} \sum_{j=1, j \neq i}^{N_s} \beta'_{ij}, \quad \text{with } \beta'_{ij} = \beta_{ij} w_j \frac{2 \max(w_i, w_j)}{w_i + w_j}. \quad (3)$$

where  $\beta_{ij}$  is the coagulation kernel between particle  $i$  and particle  $j$ ,  $\text{m}^3 \text{s}^{-1}$ ;  $\beta'_{ij}$  is a normalized kernel that relates not only to the states (e.g., masses) but also to the weights of the two simulation particles; and  $V$  is the volume of computational domain. Furthermore, the rate of coagulation event occurring among two simulation particles per unit volume is calculated as (Zhao & Zheng, 2009b)

$$R'_{\text{coag}} = \frac{1}{2} \sum_{i=1}^{N_s} C_i' = \frac{1}{2V^2} \sum_{i=1}^{N_s} \sum_{j=1, j \neq i}^{N_s} \beta'_{ij}. \quad (4)$$

Based on the total coagulation rate of each simulation particle, a Markov model for particle coagulation is then constructed. The DWMC method can evolve either in event-driven mode or in time-driven mode. In the event-driven mode,

the time step is specified as the waiting time between two successive events, which is inversely proportional to coagulation rate  $R'_{\text{coag}}$ :

$$\Delta t_{\text{ED},k} = \frac{1}{VR'_{\text{coag},k}} = \frac{2V}{\sum_{i=1}^{N_s} \sum_{j=1, \neq i}^{N_s} \beta'_{ij}}. \quad (5)$$

where  $\Delta t_{\text{ED},k}$  is the time-step after  $(k-1)$ -th coagulation event. In such a way, only one coagulation event occurs within  $\Delta t_{\text{ED},k}$  for the event-driven DWMC. While in the time-driven DWMC, many coagulation events may occur within a time step; however a simulation particle only participates in one coagulation event at most. We define the ratio ( $p$ ) of the number of coagulated simulation particles to the whole simulation particle number within  $\Delta t_{\text{TD},k}$ ,  $2/N_s \leq p \leq 1$ . The time-step in the time-driven DWMC is thus calculated as (Zhao et al., 2010)

$$\Delta t_{\text{TD},k} = pN_s / \sum_{i=1}^{N_s} (VC'_{i,k}) = pN_s V / \sum_{i=1}^{N_s} \sum_{j=1, \neq i}^{N_s} \beta'_{ij}. \quad (6)$$

The parameter  $p$  in the time-driven DWMC is recommended to have value of 0.01–0.05.

Within a prescribed time step the interacting particle pair(s) is (are) selected with probability  $\beta'_{ij} / \sum_i \sum_{j \neq i} \beta'_{ij}$ . Either the cumulative probabilities method or the acceptance–rejection method can be adopted to determine the coagulated pair(s) in either event-driven mode or time-driven mode. In this paper the acceptance–rejection (AR) method is highlighted because it may improve computational efficiency in some cases (e.g., with narrow size spectrum) or for some PBMC methods (e.g., the fast DWMC presented here). In the acceptance–rejection method, two randomly-selected simulation particles  $i$  and  $j$  undergo a coagulation event if the following condition is met:

$$r \leq \beta'_{ij} / \beta'_{\text{max}}. \quad (7)$$

where  $r$  is a random number from an uniform distribution in the interval  $[0, 1]$ ,  $\beta'_{\text{max}}$  is the maximum of the normalized coagulation kernel over all possible pairs. This procedure is repeated until a particle pair is accepted. It is worth noting that, even though  $\beta'_{\text{max}}$  is overestimated, the acceptance–rejection method can still implement the Markov process exactly but less efficiently.

Noting that the normal DWMC methods need double looping over all simulation particles to obtain the coagulation rate of a simulation particle, the waiting time and the maximum coagulation kernel, even though the smart bookkeeping technology (which is actually required a regional double looping) is used. This is why the computational cost is as high as  $O(N_s^2)$ . In this paper we proposed a fast DWMC method to avoid the double looping.

## 2.2. Fast differentially-weighted MC

### 2.2.1. Majorant kernel

Wagner et al. (Eibeck & Wagner, 2000, 2001) and Kraft et al. (Goodson & Kraft, 2002) have developed an efficient MC method for particle coagulation in population balance, where the majorant of coagulation kernel was introduced to calculate the coagulation probability of all particle pairs by single looping over all particles rather than double looping. Based on the majorant kernel  $\hat{\beta}_{ij}$  rather than the normal kernel  $\beta_{ij}$ , a Markov model with fictitious jumps was then constructed to simulate particle dynamics. The majorant kernel  $\hat{\beta}_{ij}$  has the following characteristics: (1)  $\hat{\beta}_{ij} \geq \beta_{ij}$  for all  $i, j$ ; (2)  $\hat{\beta}_{ij}$  can be formulated by  $\hat{\beta}_{ij} = \sum_k [h_k(i) \times g_k(j)]$  so that only single looping over all simulation particles is enough to calculate the coagulation rate; (3)  $\beta_{ij} / \hat{\beta}_{ij}$  is close to 1 as possible so that the fictitious jumps are rare. Some normal coagulation kernels and their corresponding majorant kernels which are usually faced in population balance are listed in Table 1.

It is worth noting that, although the computational cost of the efficient MCs is  $O(N_s)$ , the inevitable fictitious jumps will decelerate the MC simulation a certain extent. Different from utilizing the majorant kernel to calculate the coagulation rate with high efficiency, in the fast DWMC we utilize the characteristics of the majorant kernel to estimate the maximum value of all normalized coagulation kernels through only single looping. As known, the majorant kernel of normal coagulation kernel is usually  $\hat{\beta}_{ij} = \sum_k [h_k(i) \times g_k(j)]$ , then  $\beta_{\text{max}} \leq \hat{\beta}_{\text{max}} \leq \sum_k [\max(h_k(i)) \times \max(g_k(j))]$ , where  $\beta_{\text{max}}$  and  $\hat{\beta}_{\text{max}}$  are the maximum values of normal coagulation kernel and majorant kernel respectively. Once we obtain  $\max(h_k(i))$  and  $\max(g_k(j))$  through single looping over all simulation particles, we can estimate  $\beta_{\text{max}}$  and use it in the acceptance–rejection process to choose coagulation pairs at random.

However, in the DWMC we should estimate the maximum of normalized coagulation kernel (rather than the maximum of normal coagulation kernel). We take Brownian coagulation kernel in the free molecular regime as an example to show how to construct the corresponding weighted majorant kernel and then to estimate the maximum value of  $\beta'$ . Firstly, by setting  $a = v_i/v_j$  the majorant kernel can be transformed to

$$\hat{\beta}_{ij} = \sqrt{2} K_{\text{fm}} v_j^{1/6} (a^{2/3} + a^{1/6} + 1 + a^{-1/2}). \quad (8)$$

**Table 1**  
Some normal coagulation kernels, normal majorant kernels and weighted majorant kernels.<sup>a</sup>

Case	Formulation
Constant coagulation	
Normal kernel	$\beta_{ij} = A$
Majorant kernel	$\hat{\beta}_{ij} = A$
Weighted majorant kernel	$\hat{\beta}'_{ij} = 2Aw_j$
Linear coagulation	
Normal kernel	$\beta_{ij} = A(v_i + v_j)$
Majorant kernel	$\hat{\beta}_{ij} = A(v_i + v_j)$
Weighted majorant kernel	$\hat{\beta}'_{ij} = 2Aw_j v_j \left(1 + \frac{v_{\max}}{v_j}\right)$
Brownian coagulation in the free molecular regime	
Normal kernel	$\beta_{ij} = K_{\text{fm}}(v_i^{1/3} + v_j^{1/3})^2(v_i^{-1} + v_j^{-1})^{1/2}$
Majorant kernel	$\hat{\beta}_{ij} = \sqrt{2}K_{\text{fm}}(v_i^{1/6} + v_j^{1/6} + v_i^{2/3}v_j^{-1/2} + v_j^{2/3}v_i^{-1/2})$
Weighted majorant kernel	$\hat{\beta}'_{ij} = 2\sqrt{2}K_{\text{fm}}v_j^{1/6}w_j \left[ \left(\frac{v_{\max}}{v_j}\right)^{2/3} + \left(\frac{v_{\max}}{v_j}\right)^{1/6} + 1 + \left(\frac{v_{\min}}{v_j}\right)^{-1/2} \right]$
Brownian coagulation in the continuum regime	
Normal kernel	$\beta_{ij} = K_{\text{co}}(v_i^{1/3} + v_j^{1/3})(v_i^{-1/3} + v_j^{-1/3})$
Majorant kernel	$\hat{\beta}_{ij} = K_{\text{co}} \left( 2 + \left(\frac{v_i}{v_j}\right)^{1/3} + \left(\frac{v_j}{v_i}\right)^{-1/3} \right)$
Weighted majorant kernel	$\hat{\beta}'_{ij} = 2K_{\text{co}}w_j \left[ 2 + \left(\frac{v_{\max}}{v_j}\right)^{1/3} + \left(\frac{v_{\min}}{v_j}\right)^{-1/3} \right]$
Brownian coagulation in the transition regime	
Normal kernel	$\beta_{ij} = \left(\frac{1}{\rho_i^{\text{st}}} + \frac{1}{\rho_j^{\text{st}}}\right)^{-1}$
Majorant kernel	$\hat{\beta}_{ij} = \begin{cases} \hat{\beta}_{ij}^{\text{fm}}, & (\hat{R}_{ij}^{\text{fm}} \leq R^{\text{sf}}) \\ \hat{\beta}_{ij}^{\text{sf}}, & (\hat{R}_{ij}^{\text{fm}} > R^{\text{sf}}) \end{cases}$
Weighted majorant kernel	$\hat{\beta}'_{ij} = \left(\frac{1}{\rho_i^{\text{st}}} + \frac{1}{\rho_j^{\text{st}}}\right)^{-1}$

<sup>a</sup> A is a constant number;  $K_{\text{fm}} = (3/4\pi)^{1/6}(6k_B T/\rho_p)^{1/2}$ ;  $K_{\text{co}} = 2k_B T/3\mu$ ;  $k_B$  is Boltzmann's constant;  $T$  is the thermodynamics temperature of the medium;  $\rho_p$  is the density of the particles; and  $\mu$  is the viscosity of the medium. Brownian coagulation kernel in the slip flow regime is  $\beta_{ij}^{\text{sf}} = K_{\text{co}}(v_i^{1/3} + v_j^{1/3})[(C_i/v_i^{1/3}) + (C_j/v_j^{1/3})]$ ,  $\beta_{ij}^{\text{sf}} = 2K_{\text{co}}w_j C_j [1 + ((C_{\text{max}}/C_j) + (v_{\text{max}}/v_j)^{1/3}) + (C_{\text{max}}/C_j)(v_j/v_{\text{min}})^{1/3}]$ , the slip correction factor  $C_j = 1 + 2.514\lambda(6v_j/\pi)^{-1/3}$ ,  $C_{\text{max}} = 1 + 2.514\lambda(6v_{\text{min}}/\pi)^{-1/3}$ ;  $\beta_{ij}^{\text{fm}}$  is the Brownian coagulation kernel in the continuum regime;  $\lambda$  is the mean free path of the medium,  $R^{\text{sf}} = \sum_{i \neq j} \beta_{ij}^{\text{sf}}$ ,  $\hat{R}^{\text{fm}} = \sum_{i \neq j} \hat{\beta}_{ij}^{\text{fm}}$  (Kazakov & Frenklach, 1998; Patterson et al., 2006).

With the correlation  $(2w_j \max(w_i, w_j)/(w_i + w_j)) \leq a = (v_i/v_j) \leq (v_{\text{max}}/v_j)$  ( $v_{\text{min}}$  and  $v_{\text{max}}$  are the minimum and maximum volumes of particles respectively), we get

$$\hat{\beta}'_{ij} = \sqrt{2}K_{\text{fm}}v_j^{1/6}(a^{2/3} + a^{1/6} + 1 + a^{-1/2}) \leq \sqrt{2}K_{\text{fm}}v_j^{1/6} \left[ \left(\frac{v_{\text{max}}}{v_j}\right)^{2/3} + \left(\frac{v_{\text{max}}}{v_j}\right)^{1/6} + 1 + \left(\frac{v_{\text{min}}}{v_j}\right)^{-1/2} \right]. \tag{9}$$

Knowing  $(2w_j \max(w_i, w_j)/(w_i + w_j)) \leq 2w_j$ , then

$$\beta'_{ij} = \beta_{ij} \left(\frac{2w_j \max(w_i, w_j)}{w_i + w_j}\right) \leq \hat{\beta}_{ij} \left(\frac{2w_j \max(w_i, w_j)}{w_i + w_j}\right) \leq 2\hat{\beta}_{ij}w_j. \tag{10}$$

So we can define the weighted majorant kernel as the following:

$$\hat{\beta}'_{ij} = 2\sqrt{2}K_{\text{fm}}v_j^{1/6}w_j \left[ 1 + \left(\frac{v_{\text{max}}}{v_j}\right)^{1/6} + \left(\frac{v_{\text{max}}}{v_j}\right)^{2/3} + \left(\frac{v_{\text{min}}}{v_j}\right)^{-1/2} \right]. \tag{11}$$

Now it is easy to obtain the maximum of weighted majorant kernel ( $\hat{\beta}'_{\text{max}}$ ) only through the single looping. It is noted that the weighted majorant kernel  $\hat{\beta}'_{ij}$  also has the following characteristics (like the normal majorant kernel): (1)  $\hat{\beta}'_{ij} \geq \beta'_{ij}$  for all  $i, j$ ; (2)  $\hat{\beta}'_{ij}$  is only related to internal variables of one simulation particle (rather than particle pair), i.e.,  $\hat{\beta}'_{ij} = \sum_k [f_k(j)]$ , so that only single looping over all simulation particles is enough to estimate the maximum value over all  $\beta'_{ij}$ ; and (3)  $\hat{\beta}'_{\text{max}}/\beta'_{\text{max}}$  is close to 1 as possible so that the AR process choosing coagulation pair(s) is highly efficient. Table 1 summarizes these weighted majorant kernels (only for the differentially-weighted MC) for some typical cases.

2.2.2. Numerical realization of fast-DWMC

As described above,  $\hat{\beta}'_{\max}$  approximates the maximum of  $\beta'_{ij}$ .  $\hat{\beta}'_{\max}$  is then used in the AR method to choose coagulation pair(s). Before accepting a coagulation pair there may be many particle pairs that are rejected. The whole AR process includes  $N_{AR}$  particles pairs, which are chosen at random. We can thus view the AR process as a random sampling process from particle population, and the average coagulation probability of all particle pairs involved in the AR process can approximate the real average coagulation probability of all possible pairs. Based on this we can calculate the approximate time step in the fast-DWMC as the following:

$$\Delta t_{ED,k} = \frac{2V}{\sum_{i=1}^{N_s} \sum_{j=1, j \neq i}^{N_s} \beta'_{ij}} = \frac{2V}{N_s(N_s-1)\bar{\beta}'_{ij}} \approx \frac{2VN_{AR}}{N_s(N_s-1)\sum_{q=1}^{N_{AR}} \beta'_{ij,q}} \tag{12}$$

$$\Delta t_{TD,k} = \frac{pN_sV}{\sum_{i=1}^{N_s} \sum_{j=1, j \neq i}^{N_s} \beta'_{ij}} = \frac{pV}{(N_s-1)\bar{\beta}'_{ij}} \approx \frac{pVN_{AR}}{(N_s-1)\sum_{q=1}^{N_{AR}} \beta'_{ij,q}} \tag{13}$$

where  $\beta'_{ij,q}$  is the normalized coagulation kernel for the  $q$ -th particle pair in the AR process. Then the fast DWMC simulation runs as the normal DWMC to determine coagulation dynamics. The flowchart of the fast DWMC is shown in Fig. 1.

It must be emphasized that  $\hat{\beta}'_{\max}$ , which overestimates the maximum of normalized coagulation kernel  $\beta'$  to a certain extent, has obvious influence on the performance of the fast DWMC method. On the one hand, if  $\hat{\beta}'_{\max}$  is seriously

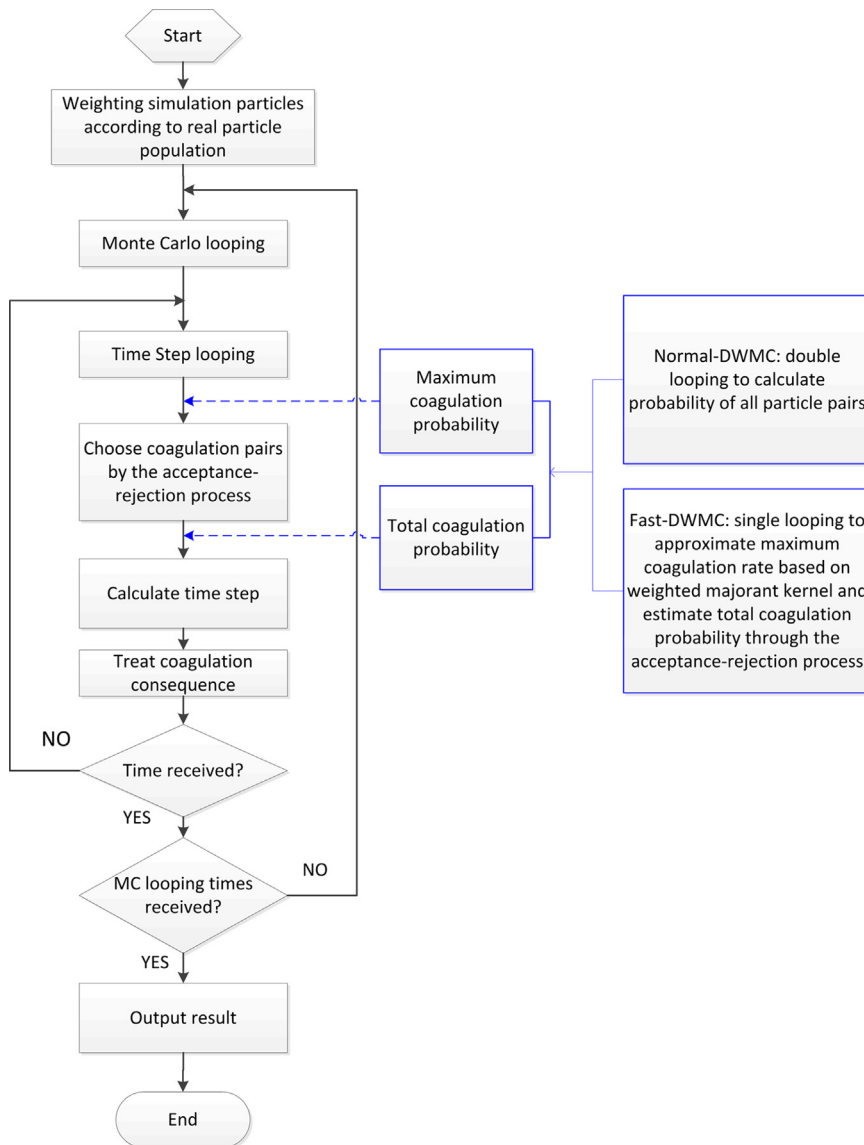


Fig. 1. The flowchart of fast-DWMC and normal-DWMC methods.

overestimated (for example, 10,000 times of  $\beta'_{\max}$ ), a large number of rejection events will occur and then lead to a significant increase in computational cost. It is validated that these formulas of weighted majorant kernel shown in Table 1 can ensure  $\hat{\beta}'_{\max}$  appropriately approximate  $\beta'_{\max}$ . Usually,  $\hat{\beta}'_{\max}/\beta'_{\max} < 10$  for Brownian coagulation cases shown in Section 3. On the other hand, in order to approximate the waiting time as accurately as possible (as shown in Eqs. (12) and (13)), it is required to have enough randomly-selected particle pairs in the AR process, which usually depends on  $\hat{\beta}'_{\max}$ . In this paper it is constrained that  $N_{\text{AR}} \geq 100$  in the event-driven mode and  $N_{\text{AR}} \geq 1000$  in the time-driven mode.

### 3. Numerical simulation and discussions

We simulated the simplest cases (constant kernel) initially with monodisperse and polydisperse distributions, a quite simplified case (linear kernel) and two physically realistic cases (Brownian coagulation in the continuum regime and free molecular regime) to examine the efficiency of the fast-DWMC and validate its accuracy comprehensively. It is easy to calculate the maximum coagulation kernel once the maximum weight and particle size are obtained in the DWMC. No special majorant kernel is required. However, it is necessary to validate the waiting time which is estimated in the fast-DWMC by summing the coagulation kernels of rejected and accepted particle pairs. On the other side, for the linear kernel case, the weighted kernel in the DWMC is related to both particle size and particle weight and can be described as  $\beta'_{ij} = \beta_{ij} w_j (2 \max(w_i, w_j) / (w_i + w_j))$ . The particle with the maximum size as well as the maximum weight may not exist. So, if we just obtain the maximum weight and the maximum size over all particles, the estimated maximum kernel may largely exceed the actual maximum kernel  $\beta'_{\max}$ , resulting in inefficiency of the acceptance–rejection process.

Particle size distribution function (PSDF) and particle number concentration  $N$  (the zero-order moment of PSDF) are gained. Cases 1–5 are described in Table 2, where  $v_0$  is the initial particle volume,  $N_0$  is the initial number concentration of real particles, and  $\tau_{\text{coag}}$  is the characteristic coagulation time. In order to fatigue against statistical noise, MC simulation is repeated three times.

#### 3.1. Computational cost

Two typical PBMC methods (the constant-N method (Smith and Matsoukas, 1998) and the stepwise Constant-V method (Kruis et al., 2000)), whose computational cost is proportional to  $O(N_s^2)$  even with smart bookkeeping technique to update the coagulation rate simultaneously, have been applied in many fields. In this paper, comparisons have been made between the fast-DWMC and two typical PBMC methods to demonstrate its accuracy and efficiency. We further compared the computational efficiency of the fast-DWMC and that of other two recent proposed highly efficient PBMC methods (the majorant kernel method (Goodson & Kraft, 2002) and the fast MC method (Wei, 2013)). MC simulations run in a general desktop PC equipped with CPU of Intel(R) Core(TM)2 Quad Q8300 @2.5 GHz and memory of 4 GB. As shown in Fig. 2, the fast-DWMC attains significant efficiency improvement compared to the other two typical methods. As shown in Fig. 3 (Brownian coagulation in the free-molecular regime), it is not hard to find that the fast-DWMC method is more efficient than PBMCs from both Kraft et al. and Wei et al. Factually, the fast-DWMC method accelerates population balance stochastic modeling comprehensively, from the calculation of the maximum coagulation kernel, the estimation of the waiting time, and the updating of particles information.

It is found from Fig. 2 that for the three typical MC methods the relation between CPU time ( $t_{\text{CPU}}$ ) and simulation particle number  $N_s$  can be generally formulated by

$$t_{\text{CPU}} \simeq a N_s^b, \quad (14a)$$

$$\frac{t_{\text{CPU,normal}}}{t_{\text{CPU,fast}}} \simeq c N_s^d, \quad (14b)$$

$$\frac{t_{\text{CPU,normal}}}{t_{\text{CPU,bookkeeping}}} \simeq e. \quad (14c)$$

where  $a$ ,  $b$ ,  $c$ ,  $d$ , and  $e$  are constant numbers, which depend on simulation cases, MC methods and even computational environment. These parameters are concluded in Table 3.

**Table 2**  
Cases description.<sup>a</sup>

Case	$v_0$	$N_0$	$\tau_{\text{coag}}$	$\beta(u, v)$
1	1	$1.0 \times 10^{10}$	$1/(N_0 A)$	$A$
2	1	$1.0 \times 10^{10}$	$1/(N_0 A)$	$A(u+v)$
3	$v_{g0} = 0.029 \mu\text{m}^3$	$10^6 \text{cm}^{-3}$	1561.3 s	$6.405 \times 10^{-10} \text{cm}^3 \text{s}^{-1}$
4	$1.414 \times 10^{-26} \text{m}^3$	$1.0 \times 10^{17}$	$1/(N_0 K_{\text{fm}} v_0^{1/6})$	$K_{\text{fm}}(u^{1/3} + v^{1/3})^2(u^{-1} + v^{-1})^{1/2}$
5	$6.545 \times 10^{-20} \text{m}^3$	$1.0 \times 10^{22}$	$1/(N_0 K_{\text{co}})$	$K_{\text{co}}(u^{1/3} + v^{1/3})(u^{-1/3} + v^{-1/3})$

<sup>a</sup>  $A = 1.0 \times 10^{-10} \text{m}^3 \text{s}^{-1}$ ,  $K_{\text{fm}} = (3/4\pi)^{1/6} (6k_B T / \rho_p)^{1/2}$ ,  $K_{\text{co}} = 2k_B T / 3\mu$ ,  $T = 300 \text{K}$ ,  $k_B = 1.38 \times 10^{-23} \text{J/K}$ ,  $\rho = 1000 \text{kg/m}^3$ ,  $\mu = 1.832 \times 10^{-5} \text{Pa s}$ .

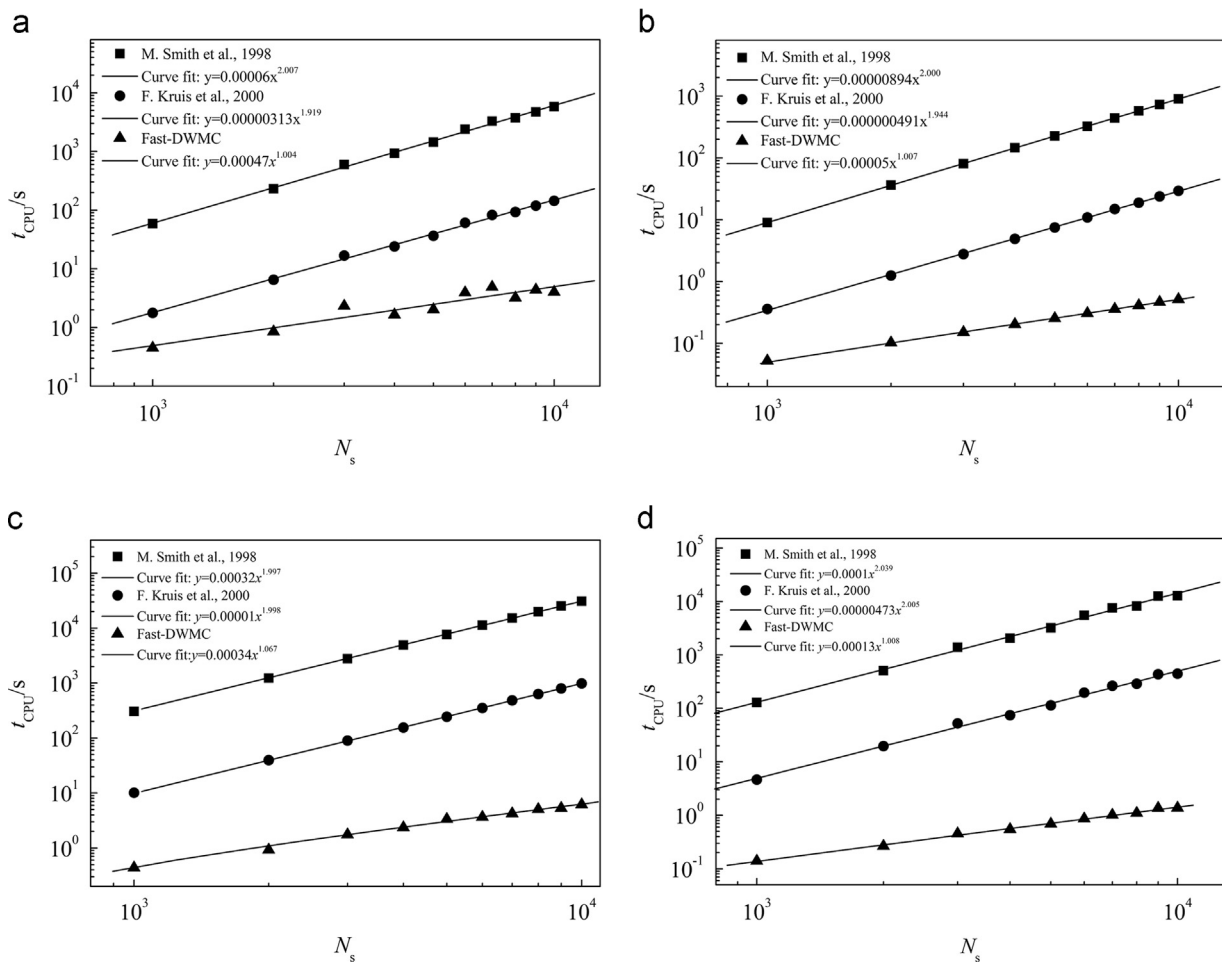


Fig. 2. CPU time vs simulation particle number for (a) Case 1; (b) Case 2; (c) Case 4; and (d) Case 5.

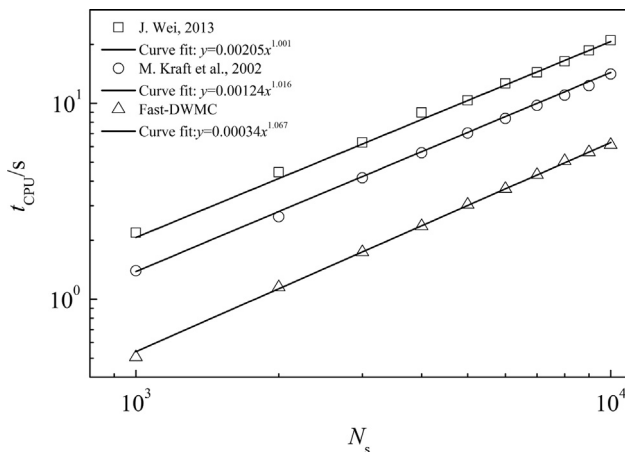


Fig. 3. CPU time vs simulation particle number for three fast methods (Brownian kernel in the free molecular regime).

It is obvious that the computational cost of normal MC methods (including the constant number method, the stepwise constant-volume method with smart bookkeeping technology and other MCs) is as high as  $O(N_s^2)$ , while the cost of the fast-DWMC is only  $O(N_s)$ . The larger the number of simulation particles, the larger the speed-up ratio. For example, with respect to Brownian coagulation in the continuum regime, when  $N_s = 10,000$  the fast-DWMC can achieve 9000 times speed-up ratio compared to the constant-number method.

**Table 3**  
Relationship between  $t_{\text{CPU}}$  and  $N_s$ .

MC methods	$a$	$b$	$c$	$d$	$e$
Constant number method	$10^{-6}-10^{-4}$	$\approx 2$	0.1–1	$\approx 1$	30–40
Smart bookkeeping technology	$10^{-7}-10^{-5}$	$\approx 2$			
Fast-DWMC	$10^{-5}-10^{-4}$	$\approx 1$			

### 3.2. Computational accuracy

To compare the relative performance and quantify numerical errors, we compare the different MC methods on a quantitative basis. For cases in which analytical solutions exist (i.e., Cases 1 and 2), the mean standard deviation  $\sigma_\xi(t)$  of the parameter  $\xi$  (number concentration  $N$  or particle size distribution function which is expressed in terms of  $P_k$  (the probability of obtaining a cluster containing  $k$  primary particles)) for three MC simulations with respect to the analytical solutions are calculated according to (Zhao et al., 2007; Zhao & Zheng, 2009a)

$$\sigma_N(t) = \frac{1}{Q} \sum_{i=1}^Q \sqrt{\frac{1}{t} \int_0^t \left[ \frac{N^{\text{MC}(i)}(t) - N^{\text{AS}}(t)}{N^{\text{AS}}(t)} \right]^2 dt}, \quad (15)$$

$$\sigma_d(t) = \frac{1}{Q} \sum_{i=1}^Q \sqrt{\frac{1}{t(v_{\text{max}} - v_{\text{min}})} \int_0^t \int_{v_{\text{min}}}^{v_{\text{max}}} (P_k^{\text{AS}}(t) - P_k^{\text{MC}(i)}(t))^2 dv dt}. \quad (16)$$

where  $Q$  is the total number of MC repetitions ( $Q=3$  in this paper); the superscript “AS” represents the analytical solutions (Leyvraz, 2003) and “MC( $k$ )” means the numerical result of the  $k$ -th MC simulation.

For Cases 4 and 5 in which some benchmark solutions exist (e.g., two Brownian coagulation cases), we compare the normal-DWMC and fast-DWMC methods with regard to self-preserving distributions.

#### 3.2.1. Case 1: Constant coagulation kernel with initial monodispersed population

The normal-DWMC and fast-DWMC methods with time-driven mode or event-driven mode are utilized to simulate the case. Figure 4 presents the relative error of number concentration  $N(t)$ , the particle size distribution function  $P_k(t)$ , and the standard deviations of  $N(t)$  and  $P_k(t)$ . Generally, all methods keep strictly mass conversation in coagulation dynamics, and predict the number concentration and size distribution well. The relative error of  $N(t)$  increases as time evolution; however it is still constrained between  $\pm 1.5\%$  (Fig. 4(a)) and the standard deviation  $\sigma_N$  tends to stabilization (Fig. 4(b)). Similar phenomenon can be found for the size distribution. The computed  $P_k$  at  $10\tau_{\text{coag}}$  agrees well with the analytical solutions for  $k < 20$ ; however the fluctuations of the computed distributions increase at the high-end of the distribution because of the smaller number of particles in this size range ( $k > 20$ ).  $\sigma_d$  first increases sharply, and then decreases gradually to a steady value at  $100\tau_{\text{coag}}$ .

It is also obvious from Fig. 4 that the event-driven MC has higher accuracy than the time-driven MC, and the normal-DWMC is more accurate than the fast-DWMC method. This is not very surprising. The event-driven version is more accurate because events are fully uncoupled among different time steps, while the time-driven mode is faster because more events are simulated within one time step. For this case, CPU costs consumed by the four MCs are in the order: normal-DWMC with event-driven mode (abbreviation “Normal-ED” in Fig. 4) > normal-DWMC with time-driven mode (Normal-TD) > fast-DWMC with event-driven mode (Fast-ED) > fast-DWMC with time-driven mode (Fast-TD). The fast-DWMC methods obtain remarkable speed-up ratio compared to the normal-DWMC methods, at the cost of slight loss in accuracy. It can be explained by “the waiting time calculated in the normal-DWMC which is more accurate than that in the fast-DWMC”. In the fast-DWMC, the error in time step leads to the simulation process that exceeds or lags behind the real process, which makes particle number concentration and PSDF deviate slightly from the real solutions.

#### 3.2.2. Case 2: Linear coagulation kernel with initial monodispersed population

The results presented in Fig. 5 show that there is only little difference in computational accuracy between the normal- and fast-DWMC methods. With regard to the number concentration, in the initial stage (about  $t < 0.04\tau_{\text{coag}}$ ), the normal-DWMC methods perform more accurately; while  $t > 0.1\tau_{\text{coag}}$  the error in the number concentration for all methods practically collapses onto a single curve that increases slowly with time (as shown in Fig. 5(b)). It depicts that all methods yield nearly identical error in the number concentration as time evolves, although there is evident difference in relative error of number concentration (as shown in Fig. 5(a)). Note that the relative error is less than 0.4% for all MCs. Further, the error in the size distribution is larger for the fast-DWMC methods and for the time-driven methods. The error in the size distribution shows no convergence trend for all four methods.  $\sigma_d$  in the event-driven MCs tends to steady states however continues to decline in the time-driven MCs when  $t > 0.1\tau_{\text{coag}}$ .

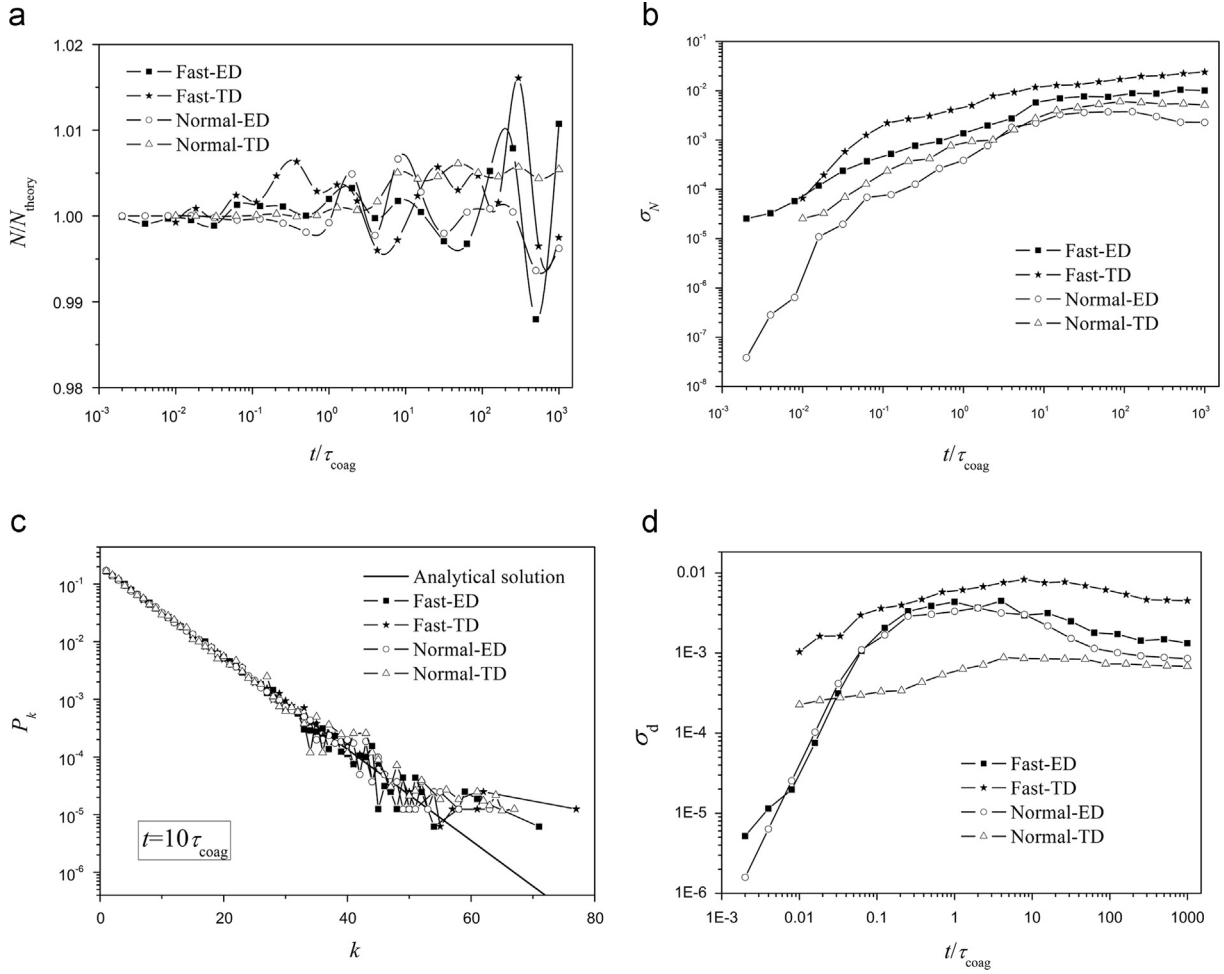


**Fig. 4.** Constant coagulation kernel case: (a) number concentration; (b) error in number concentration; (c) size distributions; and (d) error in size distributions.

The different trends of  $\sigma_N$  and  $\sigma_d$  for different MCs in Cases 1 and 2 should be ascribed to case difference. In Case 1, the weighted normalized kernel and majorant kernel are related only to the weight of simulation particle; however they are related to both the weight and size in Case 2. As time evolves the sizes and weights among simulation particles differ more and more. So  $\hat{\beta}'_{\text{max}}$  may overestimate more than the real  $\beta'_{\text{max}}$  in Case 2, which results in more rejections in the fast-DWMC methods. As a result, for Case 2 the waiting time estimated in the fast-DWMC methods may be closer to the accurate waiting time, and then the fast-DWMC methods perform higher accuracy in Case 2 than in Case 1 (as presented in Figs. 4 and 5), at the cost of lower efficiency (as presented in Fig. 2). In conclusion, an appropriate representation of  $\hat{\beta}'$  and the resultant  $\hat{\beta}'_{\text{max}}$  are very important for the performance of the fast-DWMC methods.

### 3.2.3. Case 3: Constant coagulation kernel with initially polydispersed population

Now we test the fast-DWMC for coagulation case with initially polydispersed size distribution, in which simulation particles should be differentially weighted before MC simulation. In this case, initial particle size distribution is exponential distribution

$$n(v, 0) = N_0/v_{g0} e^{-v/v_{g0}} \quad (17)$$

where the geometric mean particle volume is  $v_{g0}$ ; all the parameters are listed in Table 2. The continuous polydispersed real particle population is discretized into 200 sections by logarithmically spaced law between the largest and the smallest sizes. Every section has at least 10 simulation particles at the beginning of MC simulation; and then the total number of simulation particles is 4040.

The numerical results of the fast-DWMC method, the normal-DWMC method and analytical solutions (Williams & Loyalka, 1991) are shown in Fig. 6. It is found that the two methods can capture the first two moments (i.e., number

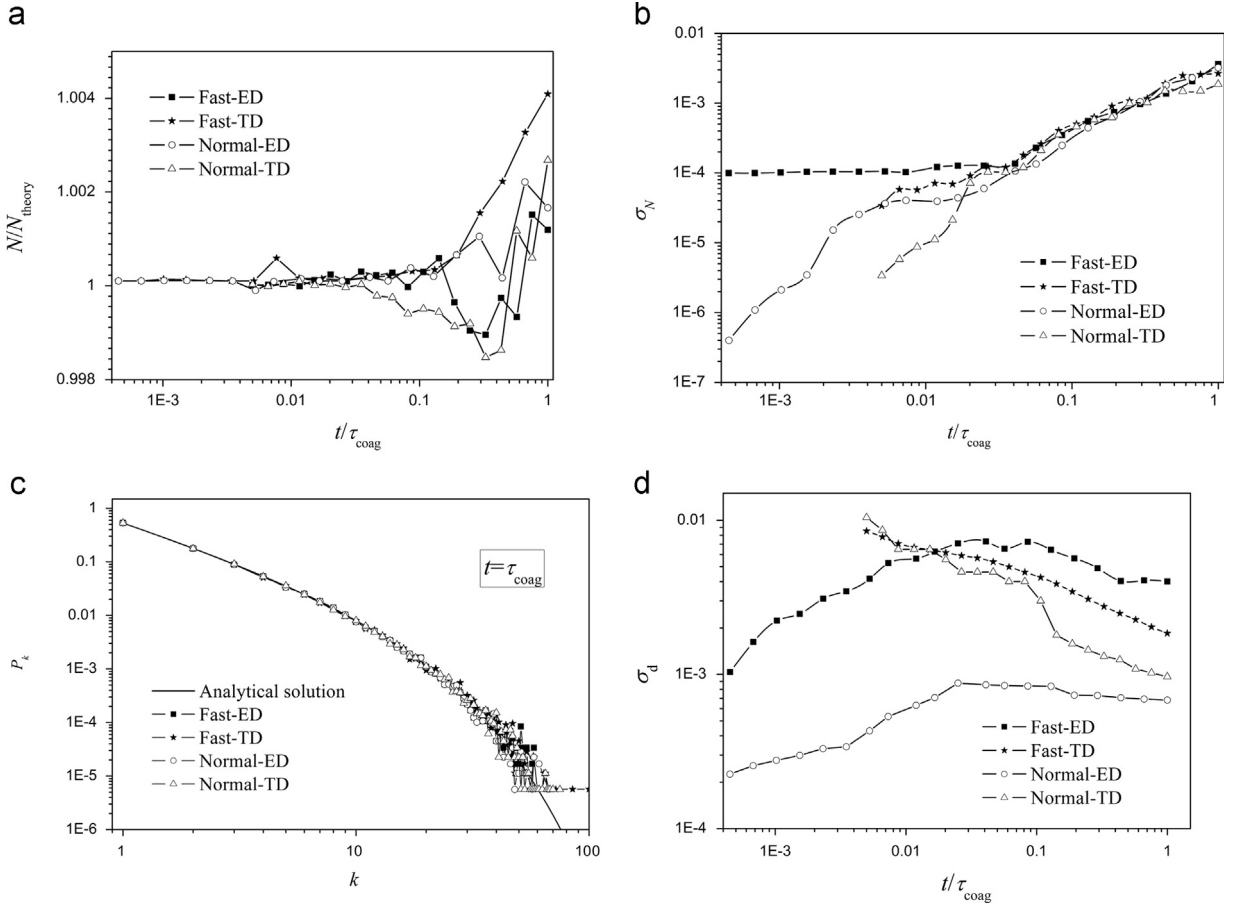


**Fig. 5.** Linear coagulation kernel case: (a) number concentration; (b) error in number concentration; (c) size distributions; and (d) error in size distributions.

concentration  $N$  and mass concentration  $M$ ) and particle size distribution function very well. With regard to number concentration and mass concentration, there are only slight differences between the two DWMC methods (as shown in Fig. 6(a)). The errors in  $N$  and  $M$  from the fast-DWMC are slightly greater than these from the normal-DWMC (as shown in Fig. 6(b)). With regard to the size distribution, it is difficult to select a better MC method from the results at  $t = 10\tau_{\text{coag}}$  (shown in Fig. 6(c)). The PSD results from the fast-DWMC and normal-DWMC oscillate around the analytical solutions.

### 3.2.4. Cases 4 and 5: Brownian coagulation with initial monodispersed population

Although no analytical solution exists for Brownian coagulation in the continuum and free molecular regimes, the discrete-sectional models (Vemury & Pratsinis, 1995) provided classical benchmark solutions of self-preserving particle size distributions. In the self-preserving formulation (Friedlander & Wang, 1966), the dimensionless particle size is defined as  $\eta = v/\bar{v} = Nv/M$ , and the dimensionless number distribution function as  $\psi = Mn(v, t)/N^2$ , where  $\bar{v}$  is the average volume,  $N$  and  $M$  are the number and mass concentrations respectively.

The simulation parameters of the two cases are listed in Table 2. Generally all MC methods simulate the self-preserving size distributions very well. The normal-DWMC and fast-DWMC methods show similar performance within the size range from  $0.01\bar{v}$  to  $10\bar{v}$ . However, at the two edges of size distributions for the two cases, the results of the fast-DWMC methods deviate obviously from the benchmark solutions and that of the normal-DWMC methods. We still ascribe the accuracy loss in the fast-DWMC to error in time-step. With respect to each discrete time-step and the total evolution time (which is the accumulation of discrete time-step), we compared their differences between the fast-DWMC and the normal-DWMC. The results of the normal-DWMC method is considered here as benchmark; the relative errors in time step and evolution time are defined as

$$\delta_{\Delta t} = \frac{|\Delta t_F - \Delta t_N|}{\Delta t_N}, \quad (18)$$

$$\delta_t = \frac{|t_F - t_N|}{t_N}. \quad (19)$$

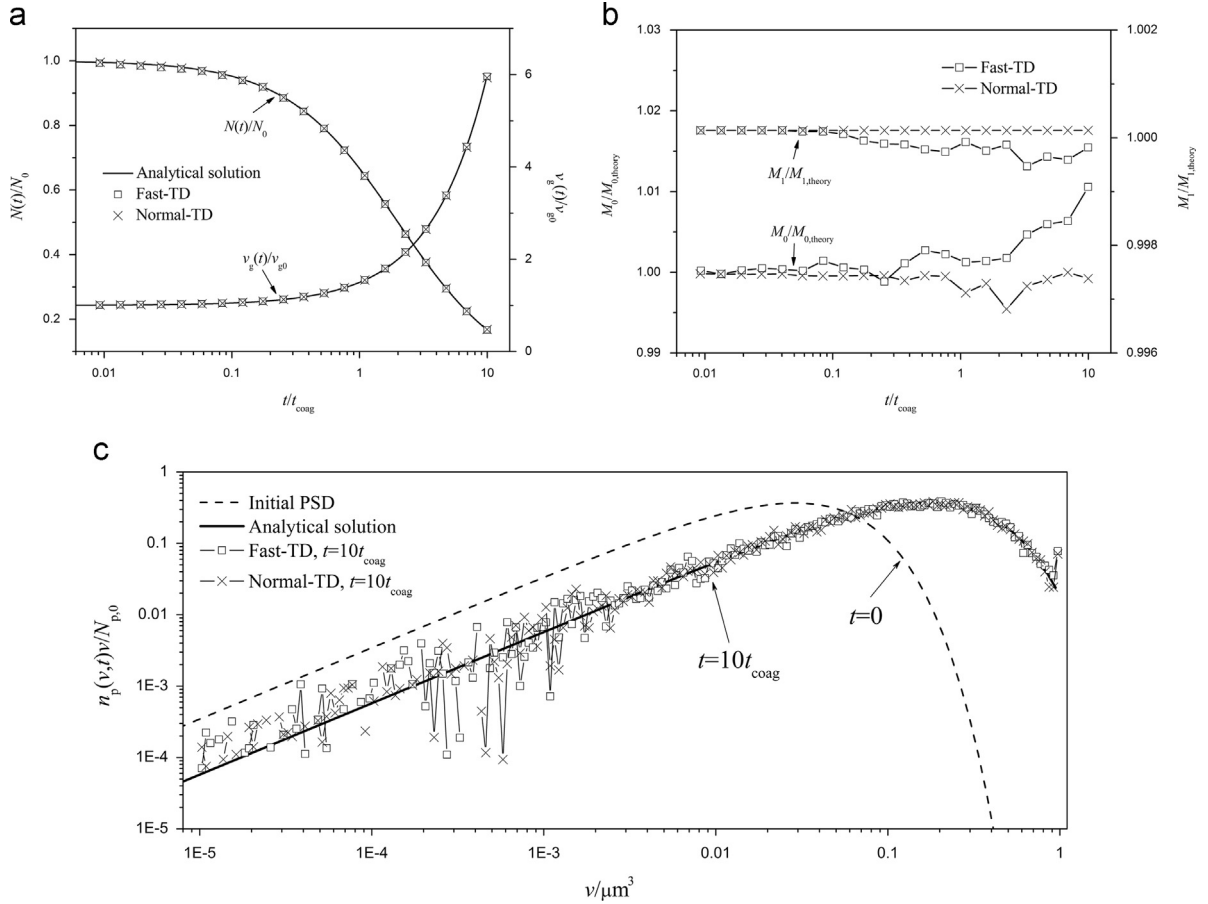


**Fig. 6.** Constant coagulation kernel with initial exponential distributed population (Case 3); (a) the time evolution of number concentration and geometric mean size; (b) error in number concentration and mass concentration; and (c) the time evolution of PSD.

where  $\Delta t_F$  and  $\Delta t_N$  are the calculated time step in the fast-DWMC and normal-DWMC methods respectively;  $t_F$  and  $t_N$  are the corresponding evolution time. The two relative errors are presented in Fig. 7(c) and (d) (for Case 4) and in Fig. 8(c) and (d) (for Case 5). It is found that the relative errors in time step are comparatively larger and more fluctuating. The relative error in time step is limited within 5% for Case 4 and 3% for Case 5. The relative errors in evolution time fluctuate around 0.15% for the two cases. Considering that the fast-DWMC can obtain speed-up ratio of about 10,000 (for 10,000 simulation particles), slight loss in accuracy is totally worthy.

The fast-DWMC can improve efficiency greatly, at the same time guarantee accuracy favorably. The good performance of the fast-DWMC methods is ascribed to appropriate choice of the weighted majorant kernel in nature. Both the normalized kernel  $\beta_{ij}$  and the weighted majorant kernel  $\tilde{\beta}_{ij}$  relate to particle size and weight, which both change during MC simulation. In order to keep appropriate rejection numbers in the AR process to achieve nice trade-off between computational cost and computational accuracy, it is necessary to keep the ratio ( $\theta$ ) of  $\tilde{\beta}'_{max}$  to  $\beta'_{max}$  within a stable range. The ratios  $\theta (= \tilde{\beta}'_{max}/\beta'_{max})$  for the two cases are presented in Figs. 7(b) and 8(b). The ratio in the Brownian coagulation case in the free molecular regime fluctuates around about 1.3, except for the initial stage ( $\theta=2$  here). And for the Brownian coagulation case in the continuum regime  $\theta$  fluctuates within 5–6, except for the initial stage ( $\theta=8$  here). The ratio  $\theta$  in Case 5 is generally greater than that in Case 4, which leads to higher accuracy (seeing relative error in time step and evolution time) while lower efficiency (shown in Fig. 2) in Case 5.

#### 4. Conclusions

As known, for a particle population with  $N_s$  simulation particles, the total number of possible coagulation pairs is  $\binom{N_s}{2} = (N_s(N_s - 1))/2$ . The normal Monte Carlo for population balance needs a double looping over all simulation particles to obtain the coagulation rate, and then calculate the waiting time between two successive events. The computational cost is

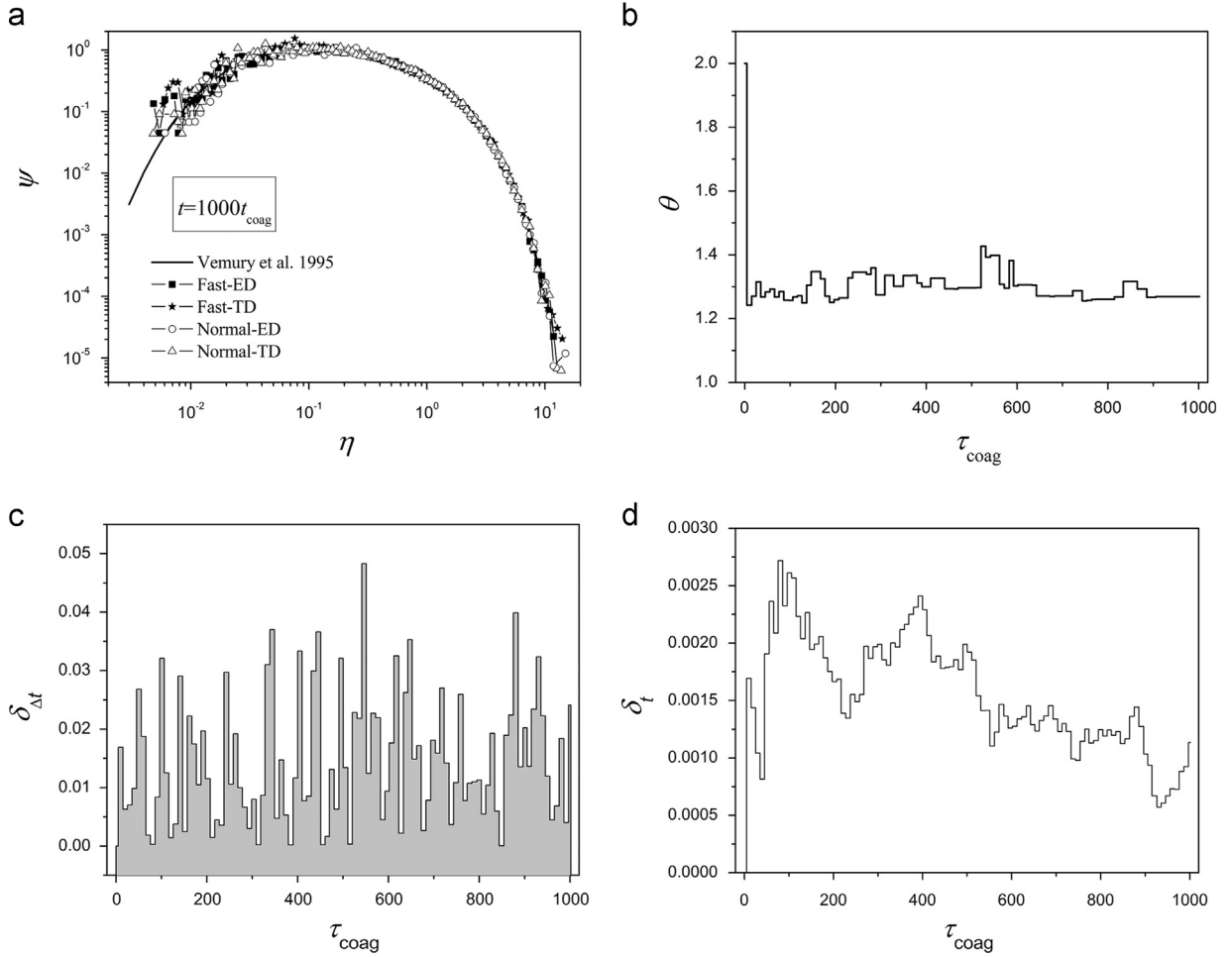


**Fig. 7.** Brownian coagulation kernel in the free molecular regime (Case 4): (a) self-preserving size distributions; (b)  $\hat{\beta}_{\text{max}}/\beta_{\text{max}}$  trends over time; (c) error in time step; and (d) error in evolution time.

thus  $O(N_s^2)$ . In order to improve MC efficiency, the particle pairs involved in the acceptance–rejection process, which are selected at random, were used to approximate a random sample of all coagulation pairs. That is, the mean of all coagulation kernels of particle pairs involved in the acceptance–rejection process was considered as the mean coagulation kernels of all possible coagulation pairs. The coagulation rate and the waiting time were thus calculated from the approximated mean coagulation kernel. The key issue of efficient PBMC was how to approximate the maximum coagulation kernel with low cost. The majorant was introduced to transform a traditional coagulation kernel to a majorant kernel, in such a way that the maximum value of this majorant kernel was obtained by only a single looping over all simulation particles. In this paper we aimed for the fast simulation of differentially-weight Monte Carlo, and thus proposed a method to construct the weighted majorant kernel (which relates to particle size and weight). Numerical tests showed the ratio of the maximum weighted majorant kernel to the maximum normalized coagulation kernel is kept within a stable range, which is essential for high accuracy and high efficiency of the fast-DWMC method. In order to test the performance of the fast-DWMC method, five special coagulation cases for which analytical solutions or benchmark solutions exist were simulated. Simulation results showed the CPU time required was only  $O(N_s)$ , and very remarkable speed-up ratio was achieved. At the same time, the errors in time step, evolution time, and accordingly, number concentration, mass concentration, and particle size distribution function were within acceptable ranges (there were only slight loss in accuracy compared to the normal-DWMC method). On the whole, the fast-DWMC method presented here can achieve nice trade-off between the computational accuracy and cost, which is usually impossible for the normal DWMC methods.

The fast-DWMC method can be extended easily to simulate single-particle events (for example, surface growth/dissolution, deposition, breakage, etc.) and nucleation. And the method is also very suitable for multivariate and multi-dimensional population balance modeling. Furthermore, it is also possible to utilize similar ideas in classical direct simulation Monte Carlo for gas dynamics to improve computational efficiency.

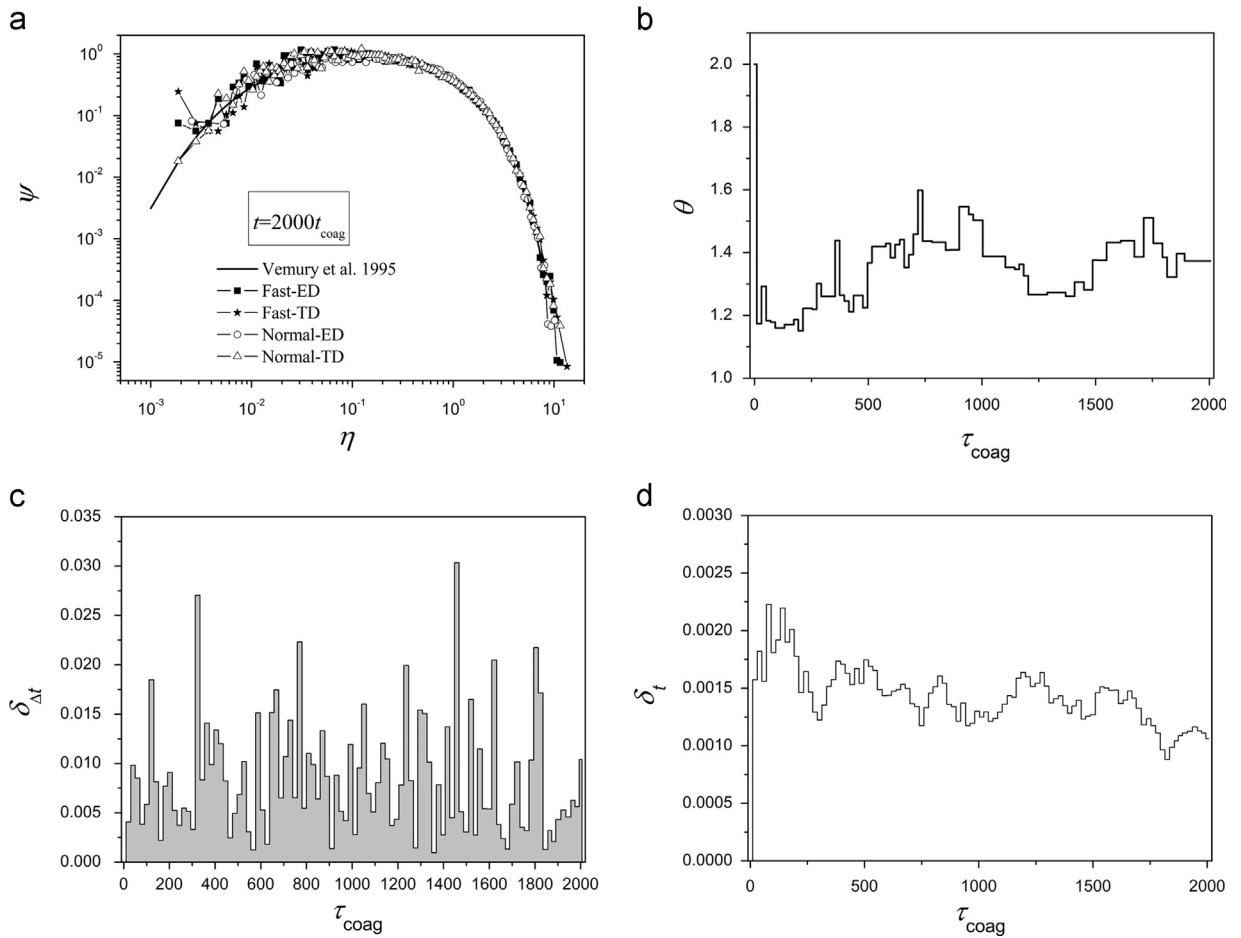


**Fig. 8.** Brownian coagulation kernel in the continuum regime (Case 5): (a) self-preserving size distributions; (b)  $\beta'_{\max}/\beta_{\max}$  trends over time; (c) error in time step; and (d) error in evolution time.

## Acknowledgments

This work was supported by the “National Natural Science Foundation of China” (51276077 and 51390494), “Program for New Century Excellent Talents in University” (NCET-09-0395), and “Open Project of State Key Laboratory of Multiphase Complex Systems (Grant no. MPCSS-2011-D-02)”.

## References

- Debyr, E., Sportisse, B., & Jourdain, B. (2003). A stochastic approach for the numerical simulation of the general dynamics equation for aerosols. *Journal of Computational Physics*, 184, 649–669.
- DeVille, R.E.L., Riemer, N., & West, M. (2011). Weighted Flow Algorithms (WFA) for stochastic particle coagulation. *Journal of Computational Physics*, 230, 8427–8451.
- Eibeck, A., & Wagner, W. (2000). An efficient stochastic algorithm for studying coagulation dynamics and gelation phenomena. *SIAM Journal on Scientific Computing*, 22, 802–821.
- Eibeck, A., & Wagner, W. (2001). Stochastic particle approximations for Smoluchowski's coagulation equation. *The Annals of Applied Probability*, 11, 1137–1165.
- Frenklach, M., & Harris, S.J. (1987). Aerosol dynamics modeling using the method of moments. *Journal of Colloid and Interface Science*, 118, 252–261.
- Friedlander, S.K. (2000). *Smoke, Dust and Haze: Fundamentals of Aerosol Dynamics* 2nd ed.). Oxford university press: City190–208.
- Friedlander, S.K., & Wang, C.S. (1966). The self-preserving particle size distribution for coagulation by brownian motion. *Journal of Colloid and Interface Science*, 22, 126–132.
- García, A.L., van den Broeck, C., Aertsens, M., & Serneels, R. (1987). A Monte Carlo simulation of coagulation. *Physica A: Statistical Mechanics and its Applications*, 143, 535–546.
- Gelbard, F., Tambour, Y., & Seinfeld, J.H. (1980). Sectional representations for simulating aerosol dynamics. *Journal of Colloid and Interface Science*, 76, 541–556.
- Gillespie, D.T. (1976). A general method for numerically simulating the stochastic time evolution of coupled chemical reactions. *Journal of Computational Physics*, 22, 403–434.
- Goodson, M., & Kraft, M. (2002). An efficient stochastic algorithm for simulating nano-particle dynamics. *Journal of Computational Physics*, 183, 210–232.
- Irizarry, R. (2008a). Fast Monte Carlo methodology for multivariate particulate systems-II: PEMC. *Chemical Engineering Science*, 63, 111–121.

- Irizarry, R. (2008b). Fast Monte Carlo methodology for multivariate particulate systems—I: point ensemble Monte Carlo. *Chemical Engineering Science*, 63, 95–110.
- Kazakov, A., & Frenklach, M. (1998). Dynamic modeling of soot particle coagulation and aggregation: implementation with the method of moments and application to high-pressure laminar premixed flames. *Combustion and Flame*, 114, 484–501.
- Kruis, F.E., Maisels, A., & Fissan, H. (2000). Direct simulation Monte Carlo method for particle coagulation and aggregation. *AIChE Journal*, 46, 1735–1742.
- Kruis, F.E., Wei, J., van der Zwaag, T., & Haep, S. (2012). Computational fluid dynamics based stochastic aerosol modeling: combination of a cell-based weighted random walk method and a constant-number Monte-Carlo method for aerosol dynamics. *Chemical Engineering Science*, 70, 109–120.
- Kruis, F.E., Zhao, H., Wei, J., & Zheng, C. (2010). A parallelized population balance-Monte Carlo method for diffusion and coagulation of nanoparticles. *Proceedings of the 6th World Congress on Particle Technology*, 26–29.
- Lécot, C., & Tarhini, A. (2008). A quasi-stochastic simulation of the general dynamics equation for aerosols. *Monte Carlo Methods and Applications*, 13, 369–388.
- Lécot, C., & Wagner, W. (2004). A quasi-Monte Carlo scheme for Smoluchowski's coagulation equation. *Mathematics of Computation*, 73, 1953–1966.
- Laurenzi, I.J., & Diamond, S.L. (1999). Monte Carlo simulation of the heterotypic aggregation kinetics of platelets and neutrophils. *Biophysical Journal*, 77, 1733–1746.
- Leyvraz, F. (2003). Scaling theory and exactly solved models in the kinetics of irreversible aggregation. *Physics Reports*, 383, 95–212.
- Liffman, K. (1992). A direct simulation Monte-Carlo method for cluster coagulation. *Journal of Computational Physics*, 100, 116–127.
- Lin, Y., Lee, K., & Matsoukas, T. (2002). Solution of the population balance equation using constant-number Monte Carlo. *Chemical Engineering Science*, 57, 2241–2252.
- Maisels, A., Einar Kruis, F., & Fissan, H. (2004). Direct simulation Monte Carlo for simultaneous nucleation, coagulation, and surface growth in dispersed systems. *Chemical Engineering Science*, 59, 2231–2239.
- Patterson, R.I.A., Singh, J., Balthasar, M., Kraft, M., & Wagner, W. (2006). Extending stochastic soot simulation to higher pressures. *Combustion and Flame*, 145, 638–642.
- Riemer, N., West, M., Zaveri, R.A., & Easter, R.C. (2009). Simulating the evolution of soot mixing state with a particle-resolved aerosol model. *J. Geophys. Res.*, 114, D09202.
- Shekar, S., Menz, W.J., Smith, A.J., Kraft, M., & Wagner, W. (2012a). On a multivariate population balance model to describe the structure and composition of silica nanoparticles. *Computers and Chemical Engineering*, 43, 130–147.
- Shekar, S., Sander, M., Riehl, R.C., Smith, A.J., Braumann, A., & Kraft, M. (2012b). Modelling the flame synthesis of silica nanoparticles from tetraethoxysilane. *Chemical Engineering Science*, 70, 54–66.
- Smith, M., & Matsoukas, T. (1998). Constant-number Monte Carlo simulation of population balances. *Chemical Engineering Science*, 53, 1777–1786.
- Vemury, S., & Pratsinis, S.E. (1995). Self-preserving size distributions of agglomerates. *Journal of Aerosol Science*, 26, 175–185.
- Wei, J. (2013). A fast monte carlo method based on an acceptance-rejection scheme for particle coagulation. *Aerosol and Air Quality Research*, 13, 1273–1281.
- Wei, J., & Kruis, F.E. (2013). GPU-accelerated Monte Carlo simulation of particle coagulation based on the inverse method. *Journal of Computational Physics*, 249, 67–79.
- Williams, M.M.R., & Loyalka, S.K. (1991). *Aerosol Science: Theory and Practice*. Pergamon Press: New York.
- Zhao, H., Kruis, F.E., & Zheng, C. (2009). Reducing statistical noise and extending the size spectrum by applying weighted simulation particles in Monte Carlo simulation of coagulation. *Aerosol Science and Technology*, 43, 781–793.
- Zhao, H., Kruis, F.E., & Zheng, C. (2010). A differentially weighted Monte Carlo method for two-component coagulation. *Journal of Computational Physics*, 229, 6931–6945.
- Zhao, H., Kruis, F.E., & Zheng, C. (2011). Monte Carlo simulation for aggregative mixing of nanoparticles in two-component systems. *Industrial & Engineering Chemistry Research*, 50, 10652–10664.
- Zhao, H., Maisels, A., Matsoukas, T., & Zheng, C. (2007). Analysis of four Monte Carlo methods for the solution of population balances in dispersed systems. *Powder Technology*, 173, 38–50.
- Zhao, H., & Zheng, C. (2009a). Correcting the multi-Monte Carlo method for particle coagulation. *Powder Technology*, 193, 120–123.
- Zhao, H., & Zheng, C. (2009b). A new event-driven constant-volume method for solution of the time evolution of particle size distribution. *Journal of Computational Physics*, 228, 1412–1428.
- Zhao, H., & Zheng, C. (2011). Two-component Brownian coagulation: Monte Carlo simulation and process characterization. *Particuology*, 9, 414–423.
- Zhao, H., & Zheng, C. (2013). A population balance-Monte Carlo method for particle coagulation in spatially inhomogeneous systems. *Computers & Fluids*, 71, 196–207.
- Zhao, H., Zheng, C., & Xu, M. (2005a). Multi-Monte Carlo method for coagulation and condensation/evaporation in dispersed systems. *Journal of Colloid and Interface Science*, 286, 195–208.
- Zhao, H., Zheng, C., & Xu, M. (2005b). Multi-Monte Carlo method for particle coagulation: description and validation. *Applied Mathematics and Computation*, 167, 1383–1399.